reactions

MDPI

Article

An Upper Limit to O_2 Evolution as Test for Radical and Nonradical Mechanisms for the Fenton Reaction

Mordechai L. Kremer

Institute of Chemistry, Hebrew University, Jerusalem 91904, Israel; mordechai.kremer@mail.huji.ac.il

Abstract: The origin of an upper limit to the amount of O_2 evolved in the rapid reaction between Fe^{2+} and H_2O_2 was investigated at a high concentration of H_2O_2. Using a nonradical model, including the formation of a primary Fe^{2+}–biperoxy complex with a diminished rate of formation of the active intermediate FeO^{2+}, agreement has been reached for the first time with the experimental data obtained by Barb et al. A limited formation of O_2 requires that a finite concentration of H_2O_2 should be present in the reaction mixture when $[Fe^{2+}]$ falls to zero. It has been shown that in Barb et al.'s model the condition for such a state ($[Fe^{2+}] = 0$, $[H_2O_2] > 0$) does not exist. Free radical based models fail as mechanisms for the Fenton reaction.

Keywords: Fenton; H_2O_2; Fe^{2+}; O_2; free radicals; catalysis

check for updates

Citation: Kremer, M.L. An Upper Limit to O_2 Evolution as Test for Radical and Nonradical Mechanisms for the Fenton Reaction. *Reactions* **2021**, *2*, 301–311. https://doi.org/10.3390/reactions2030019

Academic Editors: Dmitry Yu Murzin and Victor Ryzhov

Received: 13 May 2021
Accepted: 30 August 2021
Published: 2 September 2021

1. Introduction

The question of the mechanism and intermediates in the reaction between Fe^{2+} and H_2O_2 (the Fenton reaction) has been the subject of intensive investigation for over a century [1–20]. The reaction has gained importance as a method for the elimination of industrial waste [1]. In a different field, interest is growing in the possible significance of intermediates of the reaction in processes occurring in living systems [2]. Basic questions relating to the mechanism of the reaction are, however, still open. One of them concerns the variation of the ratio of concentrations of products upon variation of concentrations of reactants. There are two processes occurring in the system: oxidation of Fe^{2+} by H_2O_2 and decomposition of H_2O_2 to O_2 and H_2O. Based on a hypothesis of Haber and Willstaetter regarding the role of free radicals in chemical reactions, Haber and Weiss have proposed a model of the mechanism of the Fenton reaction [3]. It claimed to explain the dependence of the ratio $[O_2]/[Fe^{3+}]$, on the ratio $[H_2O_2]_o/[Fe^{2+}]_o$ ($[O_2]$ is the number of moles of O_2 evolved per 1 dm^3 of reaction mixture, the symbol $[\ ]_o$ denotes initial concentration), by attributing it to a competition of the reactions of the radical OH· with Fe^{2+} and H_2O_2, respectively. According to this theory, there should be no upper limit to the amount of O_2 evolved upon increasing the ratio $[H_2O_2]/[Fe^{2+}]$ in the reaction mixture. This prediction was found to be in contradiction to the experiment. Using high $[H_2O_2]_o/[Fe^{2+}]_o$, Barb et al. observed a rapid evolution of O_2 followed by a slow one [4]. They found that using $[H_2O_2]_o \geq 0.5$ mol dm^{-3}, the amount of O_2 evolved in the rapid phase reached a limit. A revision of the Haber Weiss model was suggested by a modification of the O_2 evolution step (see further on for details). It appears, however, that in spite of this and numerous other studies, *no positive evidence has yet been provided that the revised scheme does account for the existence of an upper limit.* Since the existence of the limit is an experimental fact, it was the aim of the present study to investigate its origin and to give a quantitative explanation for it.

2. The Mechanism

Barb et al. measured the amount of O_2 gas evolved in the time interval of 0–3 min [4]. The first measurement was made at 5 s. Linear $[O_2]$ vs. time plots were obtained with positive intercepts on the $[O_2]$ axis (Figures 1 and 6 in Reference [4]). The existence of these

intercepts implied that there was a short and rapid reaction in the system before the first measurement of $[O_2]$ could be made. Since a point at 5 s on a time scale extending from zero to 3 min appears near the origin of the time scale, the intercept on the $[O_2]$ axis could be identified, in good approximation, with $[O_2]$ evolved in the rapid phase. The problem of finding a mechanism for a satisfactory interpretation of the experimental results in the rapid phase presented a serious challenge as no $[O_2]$ vs. time and $[Fe^{2+}]$ vs. time data (or their equivalents) were available in the time interval of 0–5 s, only the values of $[O_2]$ at its end in a series of experiments (experimental difficulties being due to gas evolution in the reacting solution in optical measurements, danger of explosion in a closed stopped flow apparatus, etc.). The following interpretation is based on a nonradical model [10,11]. It is presented in Figure 1. It assumes the formation of an active intermediate FeO^{2+}, formed from a precursor complex $Fe^{2+}{\cdot}H_2O_2$ (C_1). In addition, and as a modification of an earlier version of the model, it includes the formation of a biperoxy complex (C_2) yielding FeO^{2+} at a lower rate than C_1 (step 10). This extension proved to be necessary to account for the existence of a limit to the amount of O_2 formed in the reaction at high $[H_2O_2]$. Neglecting the slow step 10, the mechanism has one path for oxidizing Fe^{2+} to Fe^{3+} (reactions (1)-(3)-(5),) and two reaction cycles ((1)-(3)-(4)-(1) and (1)-(3)-(6)-(7)-(1)) for the production of O_2. Steady state has been assumed to exist for $[FeO^{2+}]$, but not for $[C_1]$ and $[C_2]$. Steady state existed necessarily for $[FeOFe^{5+}]$. Its presence in the system was discovered only when $[H_2O_2]$ was reduced to the 10^{-5} molar range [10]. A total of 10^5 fold higher $[H_2O_2]$ reduced $[FeOFe^{5+}]$ to the steady state range. Assuming negligible rate constants for the back reactions k_2, k_8, k_{11}, the following rate equations were obtained

$$d[C_1]/dt = k_1\,[Fe^{2+}]\,[H_2O_2] - (k_3 + k_9\,[H_2O_2])\,[C_1] \quad (1)$$

$$d[C_2]/dt = k_9\,[H_2O_2]\,[C_1] - k_{10}\,[C_2] \quad (2)$$

$$d[Fe^{3+}]/dt = 2\,v_R\,R2 \quad (3)$$

$$d[O_2]/dt = v_R\,(R1 + R3) \quad (4)$$

$$v_R = k_3\,[C_1] + k_{10}\,[C_2] \quad (5)$$

$$[FeO^{2+}] = v_R/(k_4\,[H_2O_2] + k_5\,[Fe^{2+}] + k_6\,[Fe^{3+}]) \quad (6)$$

$$R1 = [H_2O_2]/([H_2O_2] + (k_5/k_4)\,[Fe^{2+}] + (k_6/k_4)\,[Fe^{3+}]) \quad (7)$$

$$R2 = [Fe^{2+}]/((k_4/k_5)[H_2O_2]+[Fe^{2+}]+(k_6/k_5)[Fe^{3+}]) \quad (8)$$

$$R3 = [Fe^{3+}]/((k_4/k_6)\,[H_2O_2] + (k_5/k_6)\,[Fe^{2+}] + [Fe^{3+}]) \quad (9)$$

$$[Fe^{2+}] = [Fe^{2+}]o - [Fe^{3+}] - [C_1] - [C_2]$$

$$[H_2O_2] = [H_2O_2]o - 2\,[O_2] - 0.5\,[Fe^{3+}]$$

In the calculation of $[H_2O_2]$, $[C_1]$ and $[C_2]$ could be neglected because of the large excess of $[H_2O_2]$ over $[Fe^{2+}]$ in the experiments. The differential equations were integrated numerically by using the method of Gear. The initial value of $[Fe^{2+}]$ in the simulations was 4×10^{-2} mol dm^{-3}. To cover the range of $[H_2O_2]$ in the experiments of Barb et al. (Figure 6, pH = 1.8, T = 0 °C, [4]), seven simulation runs were performed at seven $[H_2O_2]_o$ with equal intervals between them in the range 0.5–3.5 mol dm^{-3} (among them concentrations identical with those used in the experiments). $[Fe^{3+}]$, $[C_1]$ and $[C_2]$ at time = 0 were set to zero. Trial values of rate constants k_1, k_3, k_9, k_{10}, k_4/k_5, k_6/k_5 were inserted as initial parameters. (Other rate constants appearing in the rate equations were calculated as combinations of the parameters of the basis set.) $[C_1]$, $[C_2]$, $[Fe^{3+}]$ and $[O_2]$ vs. time curves were simulated. For a successful simulation, the convergence of all $[O_2]$ vs. time curves at 5 s at the target value of 1.40×10^{-2} mol dm^{-3} (upper limit at pH = 1.8 in the experiments of Barb et al. [4]) was a necessary but not sufficient condition. As around 5 s, or before it, there is a sharp fall in the rate of O_2 evolution, the limit must be approached in all runs with diminishing slopes of the $[O_2]$ vs. time curves. To this end, simulations were continued

beyond 5 s and values obtained at 6, 7, and 8 s were also included in the summation of squared deviations of calculated values of $[O_2]$ from 1.40×10^{-2} mol dm^{-3}. The total sum of squared deviations was minimized by varying rate parameters using a combination of Migrad and Simplex minimum searching routines.

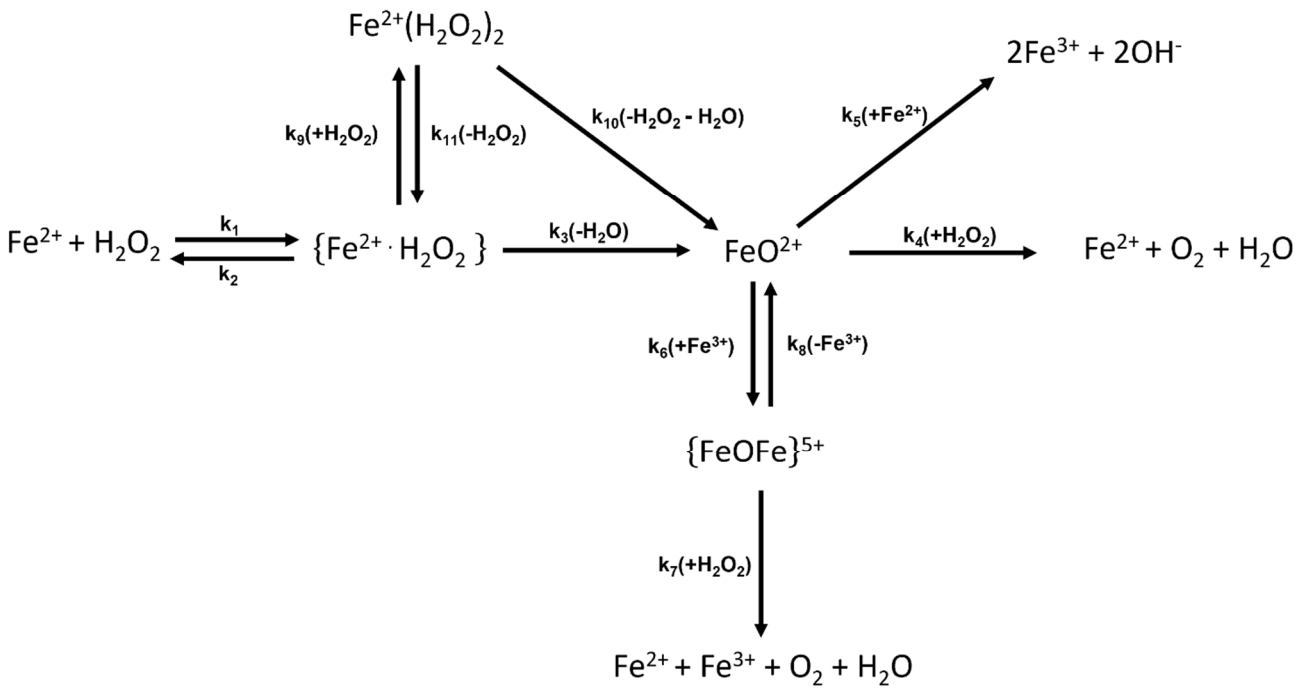

Figure 1. The nonradical mechanism.

3. Results

To calculate meaningful values of standard deviations, the number of simulations was increased to 31 by changing $[H_2O_2]_o$ between 0.5 and 3.5 mol dm^{-3} in steps of 0.1 mol dm^{-3}. The standard deviation of calculated $[O_2]$ values at 5 s from the target of 1.40×10^{-2} mol dm^{-3} was 1.4×10^{-4} mol dm^{-3}. The optimal set of rate parameters together with conditional standard deviations were: $k_1 = (3.84 \pm 0.13) \times 10$ mol^{-1} dm^3 s^{-1}, $k_3 = (1.19 \pm 0.03) \times 10^2$ s^{-1}, $k_9 = (3.16 \pm 0.04) \times 10$ mol^{-1} dm^3 s^{-1}, $k_{10} = 2.02 \times 10^{-4}$ s^{-1}, $k_4/k_5 = (2.82 \pm 0.06) \times 10^{-3}$, $k_6/k_5 = (1.52 \pm 0.05) \times 10^{-1}$. (Due to step 10 being a slow parallel path to FeO^{2+} formation, it was not possible to determine the conditional standard variation of k_{10}.) Similar values of k_1 and k_9 indicate similar energetic conditions for the first and second H_2O_2 molecules to enter the coordination sphere of Fe^{2+} ions. The difference between them appears in the rate of their decomposition to yield FeO^{2+}. Here C_2 shows more stability and consequently lower rate constant of decomposition ($k_{10} << k_3$). This difference is at the root of the existence of a limit to O_2 evolution at high $[H_2O_2]$. In Figure 2, simulated curves of $[O_2]$ vs. t are shown at $[H_2O_2]_o = 0.5$ and 3.5 mol dm^{-3}, (triangles and squares, respectively) representing the lower and upper limits of the concentration range in the experiments.

At high $[H_2O_2]$, it showed a very rapid approach (measured on the timescale of milliseconds) to an upper limit of $[O_2]$. The curve with low $[H_2O_2]$ reached the same limit in about 1.5 s. Figure 3 presents calculated (circles) and experimental (triangles) values of the amount of O_2 evolved at 5 s. Table 1 lists the numerical results.

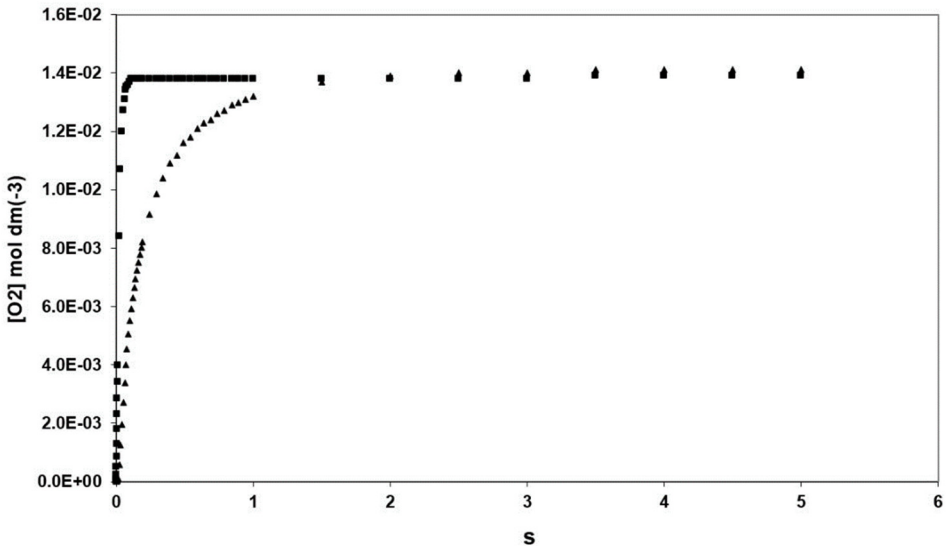

Figure 2. Simulated evolution of O_2 in the Fenton reaction.

$[Fe^{2+}]_o = 4.00 \times 10^{-2}$ mol dm^{-3}

$[H_2O_2]o = 0.5$ mol dm^{-3} (triangles)	$[H_2O_2]_o = 3.5$ mol dm^{-3} (squares)
$k_1 = 3.84 \times 10$ mol^{-1} dm^3 s^{-1}	$k_3 = 1.19 \times 10^2$ s^{-1}
$k_9 = 3.16 \times 10$ mol^{-1} dm^3 s^{-1}	$k_{10} = 2.02 \times 10^{-4}$ s^{-1}
$k_4/k_5 = 2.82 \times 10^{-3}$	$k_6/k_5 = 1.52 \times 10^{-1}$

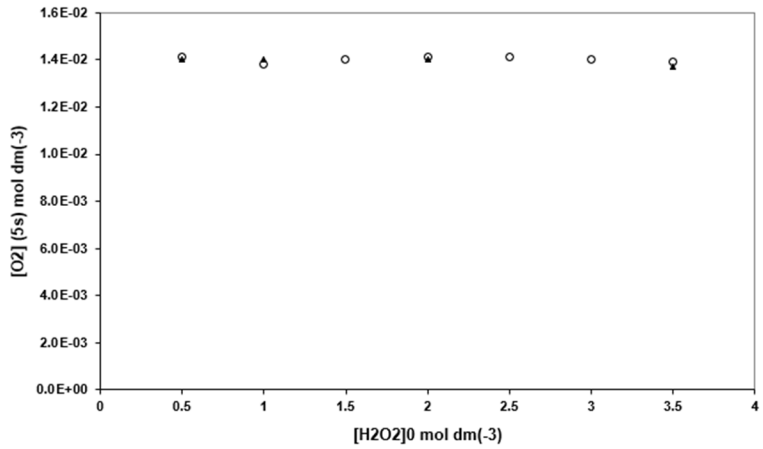

Figure 3. Simulated and experimental limiting values of $[O_2]$, Simulated values (circles), experimental values (triangles). $[H_2O_2]_o = 0.5, 1, 1.5, 2, 2.5, 3, 3.5$ mol dm^{-3}. Other parameters as in Figure 2.

Table 1. Simulated and experimental values of $[O_2]$ evolved in 5 s.

$[O_2]_{exp}$ mol dm^{-3}	$[O_2]_{sim}$ mol dm^{-3}	$[H_2O_2]_o$ mol dm^{-3}
1.40×10^{-2}	1.41×10^{-2}	0.5
1.40×10^{-2}	1.38×10^{-2}	1
—	1.40×10^{-2}	1.5
1.40×10^{-2}	1.41×10^{-2}	2
—	1.41×10^{-2}	2.5
—	1.40×10^{-2}	3
1.37×10^{-2}	1.39×10^{-2}	3.5

Standard deviation of 31 values of $[O_2]_{sim}$ from 1.40×10^{-2} mol dm^{-3} (target) = 1.38×10^{-4} mol dm^{-3}. Values of $[O_2]_{exp}$ from the work of Barb et al. ($[Fe^{2+}]_o = 4.00 \times 10^{-2}$ mol dm^{-3}, T = 0 °C, pH = 1.8, Ref. [4], Figure 6).

Data both in the Figure and in the Table show that agreement has been reached between calculated and experimental values of $[O_2]$ evolved in 5 s both showing constancy in the range of $[H_2O_2]_o$ = 0.5–3.5 mol dm^{-3}. (It may be added at this point that a previous attempt to account for the existence of the upper limit to O_2 evolved; using the nonradical model without the inclusion of C_2, was not successful [11].)

4. Discussion

To investigate the source of convergence of $[O_2]$ vs. time curves at 5 s, the terms contributing to the rate of O_2 formation were examined. These were v_R, R1, R2 and R3. By definition, R terms vary between 0 and 1, some decreasing and some increasing in the course of the reaction. Plots of the terms R1 (circles), R2 (squares) and R3 (triangles) are shown in Figure 4. (Initial conditions $[H_2O_2]_o$ = 2 mol dm^{-3} and $[Fe^{2+}]_o = 4 \times 10^{-2}$ mol dm^{-3} and $[Fe^{3+}]_o$ = 0.) Plots were obtained by entering the numerical values of the rate parameters and of their combinations into Equations (7)–(9). The following results were obtained:

1. The starting value of R1 was 0.12. It rose in 0.2 s to 0.59 and remains constant. (Although $[H_2O_2]$ is decreasing, R1 is increasing due to the steep decrease in the $[Fe^{2+}]$ term in the denominator.)
2. The starting value of R2 was 0.88. It decreased in 0.2 s to practically zero.
3. The starting value of R3 was 0. It rose in 0.2 s to 0.41 and remained constant.

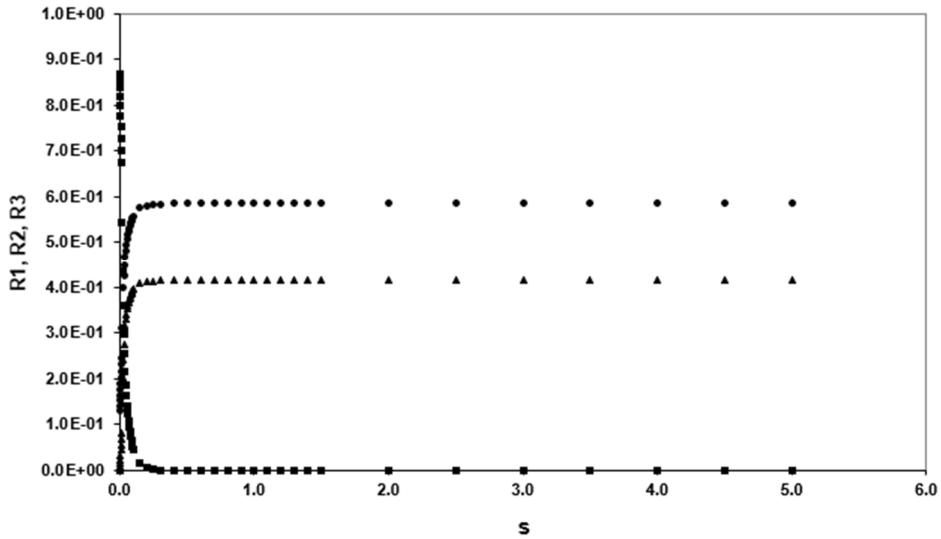

Figure 4. R terms as functions of time. R1 (circles), R2 (squares), R3 (triangles) $[H_2O_2]_o$ = 2 mol dm^{-3}. Other parameters as in Figure 2.

These results showed that, except for a short initial period, all R terms were constant during the time interval ending at 5 s. The reason for the particular shape of the $[O_2]$ vs. time curves must therefore be found in the time variation of v_R. Since $k_3 >> k_{10}$, the time variation of v_R was determined almost entirely by the time variation of $[C_1]$ but indirectly also by that of $[C_2]$. Figure 5 shows this variation. In the Figure, plots of $[C_1]$ vs. t (triangles) and $[C_2]$ vs. t (squares) are shown at $[H_2O_2]_o$ = 0.5 mol dm^{-3} (empty markers) and 3.5 mol dm^{-3} (full markers). The form of the curves in the Figure is the result of two opposing effects of $[H_2O_2]$ on the kinetics of the reaction. At high $[H_2O_2]$, the rate of formation of C_1 was high, $[C_1]$ reaching a (relatively) high maximum. Up to the maximum, conversion of C_1 into C_2 decreased the rate of increase of $[C_1]$. After the maximum, it increased the rate of decrease of C_1. The second effect was more pronounced as $[C_2]$ was higher after the maximum than before it. At low$[H_2O_2]$, there was slow accumulation of C_1 with a low maximum of $[C_1]$.

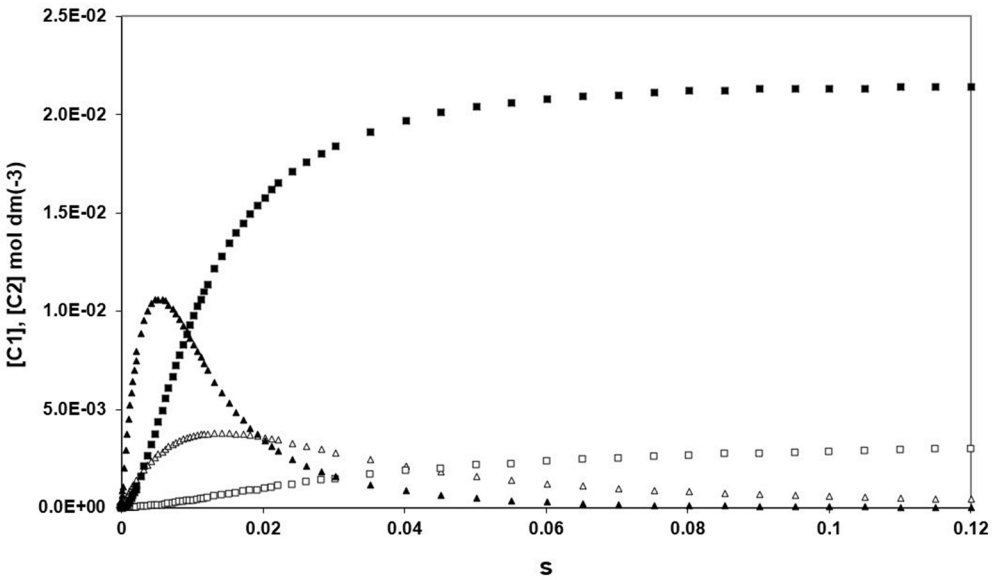

Figure 5. Kinetics of $[C_1]$ and $[C_2]$ in the early phase. $[C_1]$ (triangles), $[C_2]$ (squares); $[H_2O_2]_o$ = 0.5 mol dm^{-3} (empty symbols); $[H_2O_2]_o$ = 3.5 mol dm^{-3} (full symbols). Other parameters as in Figure 2.

There was little formation of C_2 with little retardation of the increase in $[C_1]$ and little acceleration of its decrease. Because of the rapid fall of $[C_1]$ after the maximum at a relatively high value of $[H_2O_2]$ and its damped change at low $[H_2O_2]$, *the decreasing parts of $[C_1]$* vs. *time plots a high and low $[H_2O_2]$ had a point of intersection***.** This implies, that up to the point of intersection, the rate of formation of the active intermediate FeO^{2+} ($v_R \approx k_3$ $[C_1]$) was higher with high $[H_2O_2]$, but after the point of intersection, it became relatively higher with lower $[H_2O_2]$. Since under the conditions of the experiments $[Fe^{2+}] << [H_2O_2]$, practically all FeO^{2+} will produce O_2. Therefore, v_R can be equated, in good approximation, with the rate of production O_2 (v_{O_2}). We can summarize the results of this section as follows. Denoting high and low $[H_2O_2]$ by (a) and (b), and the time interval up to and after the point of intersection by (α) and (ß), respectively, we have the following relationships between rates of evolution of O_2 in the two phases of the reaction in the time interval 0–5 s:

$$v_{O_2}(a\alpha) > v_{O_2}(b\alpha) \text{ and } v_{O_2}(a\beta) < v_{O_2}(b\beta) \quad (10)$$

This is shown in Figure 6. Full triangles represent simulations with $[H_2O_2]_o$ = 3.5 mol dm^{-3} (case a), empty triangles with $[H_2O_2]_o$ = 0.5 mol dm^{-3} (case b).

The two curves have a point of intersection at about 40 ms. The similarity between the corresponding curves of $[C_1]$ in Figure 5 and of v_{O_2} in Figure 6 is clear. The total amount of O_2 evolved at high and low $[H_2O_2]$ during the time interval 0–5 s can be written as

$$O_2(a) = O_2(a\alpha) + O_2(a\beta) \text{ and } O_2(b) = O_2(b\alpha) + O_2(b\beta) \quad (11)$$

Considering the inequalities in Equation (10), the difference in rates during phase α between case a and b are larger than the reversed differences during phase β. The duration of phase β is, however, considerably longer than that of phase α, (about 125 times longer in the present case). Thus, in case b, a lesser amount of O_2 produced during phase α may be balanced by a larger amount produced during phase β. The extent of balancing depends on the amounts of O_2 produced during phases α and β in cases a and b. The fact that in the simulations a constant amount of O_2 was calculated in all runs in 5 s proves that for the sums in Equation (11) exists

$$O_2(a\alpha) + O_2(a\beta) = O_2(b\alpha) + O_2(b\beta) = \text{constant} \quad (12)$$

The existence of an upper limit to O_2 evolved is thus due to the constancy of the sum of pairs of $O_2(x\alpha)$ and $O_2(x\beta)$ terms where x denotes any concentration of H_2O_2 between 0.5 and 3.5 mol dm^{-3}.

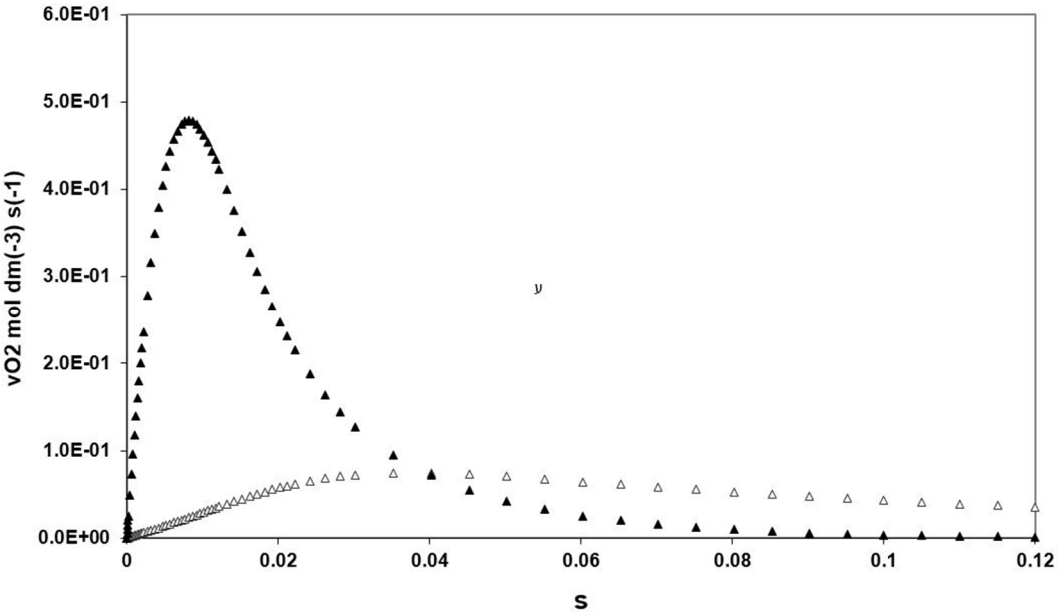

Figure 6. Rate of O_2 evolution in the early phase. $[H_2O_2]_o$ = 0.5 mol dm^{-3} (empty triangles); $[H_2O_2]_o$ = 3.5 mol dm^{-3} (full triangles). Other parameters as in Figure 2.

Figure 7 shows the variation in time of the rates of reaction in the two O_2 producing cycles denoted as v_4 and v_6, respectively. Their values are presented as empty triangles and full squares. Values of the total rate of evolution of O_2, $v_{O_2} = v_4 + v_6$, are shown as full triangles. Initially, $[Fe^{3+}] = 0$ and $v_{O_2} = v_4$; the two curves coincided. As Fe^{3+} began to be formed, the rate of the Fe^{3+} ion catalyzed path of O_2 evolution became significant too. The maximum of the total rate of formation of O_2 occurred near 20 ms, while at about 100 ms, most of the O_2 measured at 5 s had already been formed. It explains why it appeared as an initial burst (catalase burst). Reducing the concentration of $[H_2O_2]$ by a factor of 10^3 to 10^4, the role of C_2 in the mechanism became insignificant [10]. The influence of C_2 on the kinetics of C_1 at high $[H_2O_2]$ provides indirect proof of the formation of the primary intermediate C_1, until now only assumed to exist. It should be noted that the inclusion of C_2 in the mechanism implies that when using the mixture $Fe^{2+} + H_2O_2$ in oxidation of substrates, the increase in $[H_2O_2]$ beyond a certain limit decreases the efficiency of the mixture as it decreases the rate of formation of FeO^{2+}. In agreement with this prediction, Barb et al. report that "dilute solutions of methyl orange are readily oxidized to colorless compounds by 10^{-4} mol dm^{-3} Fe^{2+} and 10^{-4} mol dm^{-3} H_2O_2 to give completely colorless solutions [4]. When the hydrogen peroxide concentration is increased, the extent of this oxidation is decreased, and with 1 mol dm^{-3} H_2O_2, no destruction of color is observed" (Ref. [4], p. 464). The simulations showed only the increasing part of the $[C_2]$ vs. t curve up to a plateau. Concerning the decreasing part, the half time of decay from the maximum value can be calculated to be 58 min, a time span much longer than that in which measurements were made (3 min). Therefore, in the time range of the experiments C_2 can be regarded as an inert intermediate. The quantitative aspect of the discussion on this point is, however, only approximate, due to the difficulty of determining the value of k_{10} with sufficient accuracy.

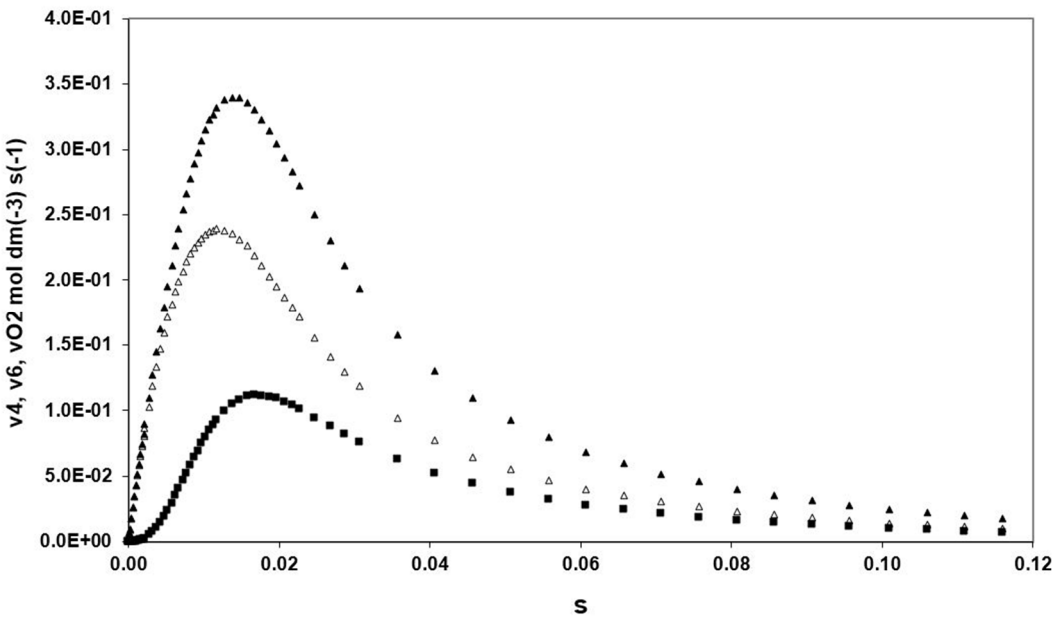

Figure 7. Resolution of the rate of O_2 evolution into H_2O_2 and Fe^{3+} dependent components. v_4 (empty triangles); v_6 (full squares); v_{O_2} (full triangles); $[H_2O_2]_o$ = 2 mol dm^{-3}; Other parameters as in Figure 2.

The concept of FeO^{2+} as intermediate in the Fenton reaction has been supported by density functional studies of Baerends and coworkers and also by Lu and coworkers. They have shown that the energetically favorable path of the reaction between Fe^{2+} and H_2O_2 led to the formation of FeO^{2+} rather than free radicals [15,16].

5. Free Radical Models of the Mechanism of the Fenton Reaction

In free radical models based on one-equivalent oxidation/reduction reactions, the precursor of O_2 is the radical $HO_2\cdot$. The first model, proposed by Haber and Weiss, consists of the following steps:

$$Fe^{2+} + H_2O_2 \rightarrow Fe^{3+} + OH\cdot + OH^- \quad (13)$$

$$OH\cdot + H_2O_2 \rightarrow HO_2\cdot + H_2O \quad (14)$$

$$HO_2\cdot + H_2O_2 \rightarrow OH\cdot + O_2 + H_2O \quad (15)$$

$$OH\cdot + Fe^{2+} \rightarrow Fe^{3+} + OH^- \quad (16)$$

It is a chain reaction in which (13) is the initiation step, (14) and (15) are chain carriers, and (16) is the chain termination step. $OH\cdot$ and $HO_2\cdot$ are free radicals derived from H_2O_2. The balance between the oxidation of Fe^{2+} and O_2 evolution depends on the ratio $r = [H_2O_2]/[Fe^{2+}]$, i.e., on the balance between reactions (14) and (16). At low r, (16) is dominant and the reaction is restricted to steps (13) and (16), resulting in oxidation of Fe^{2+} and no evolution of O_2. At increasing r, (14) begins to compete with (16) and evolution of O_2 accompanies the oxidation of Fe^{2+}, as observed experimentally. In deriving rate expressions for the formation of products, free radical intermediates are assumed to be in steady states. Their concentrations are given by the equations

$$[OH\cdot] = (k_{13}/k_{16})\,[H_2O_2] \text{ and } [HO_2\cdot] = \{k_{13}k_{14}/(k_{15}k_{16})\}\,[H_2O_2]$$

The rate of O_2 evolution becomes (Ref. [3], Equation (6))

$$d[O_2]/dt = (k_{13}k_{14}/k_{16})\,[H_2O_2]^2 \quad (17)$$

This equation cannot be the correct expression for the rate of O_2 evolution in the Fenton reaction. Namely, according to it, the rate should be no function of $[Fe^{2+}]$, thus

that of r. The model, on the other hand, requires that $d[O_2]/dt$ should approach zero with decreasing r by increasing $[Fe^{2+}]$ at a finite $[H_2O_2]$. According to Equation (14) $d[O_2]/dt$ becomes zero only for $[H_2O_2] = 0$. The rate equation is therefore not consistent with the model: the Haber Weiss scheme falls short of accounting for the course and kinetics of the Fenton reaction.

A modification of the Haber and Weiss model has been suggested by Barb et al. [4].

$$Fe^{2+} + H_2O_2 \rightarrow Fe^{3+} + OH\cdot + OH^- \quad (18)$$

$$OH\cdot + Fe^{2+} \rightarrow Fe^{3+} + OH^- \quad (19)$$

$$OH\cdot + H_2O_2 \rightarrow HO_2\cdot + H_2O \quad (20)$$

$$HO_2\cdot + Fe^{2+} \rightarrow Fe^{3+} + HO_2{}^- \quad (21)$$

$$HO_2\cdot + Fe^{3+} \rightarrow Fe^{2+} + O_2 + H^+ \quad (22)$$

The crucial change in the model is the replacement of H_2O_2 by Fe^{3+} in (22) as the O_2 producing step. With this modification, the model *ceases to be a chain reaction*. Namely, there are three pathways along which the reaction can proceed: (1) (18)-(19) (Fe^{2+} oxidation), (2) (18)-(20)-(21) (Fe^{2+} oxidation), and (3) (18)-(20)-(22) (O_2 evolution). The last one is a self-repeating cycle. The Barb model is not a chain reaction, because the initiation step (18) is part of the O_2 producing cycle. (In a chain reaction the product forming cycle cannot include the initiation step). The following description of the course of the reaction is valid for concentrations of reactants used in the experiments of Barb et al.: $[H_2O_2]_o = 0.5–3.5$ mol dm^{-3} and $[Fe^{2+}]_o = 4 \times 10^{-2}$ mol dm^{-3} [4]. Regarding rate constants, in the present context it is sufficient to note that rate constants of reactions involving free radicals (k_{19}, k_{20}, k_{21}, k_{22}) are extremely high while that of a reaction between an ion and a molecule (k_{18}) is in comparison low. The kernel of the model is the cycle consisting of (18), (20), and (22). Their sum is $2\ H_2O_2 = O_2 + 2\ H_2O$. It presents the path for the decomposition of H_2O_2. Fe^{2+} and Fe^{3+} ions participate in these reactions but are cancelled out in the summation. It means that they are neither formed nor consumed in the cycle; their concentrations remain constant. Thus, the cycle of the three reactions presents a scheme for the catalytic evolution of O_2 by the pair Fe^{3+}–Fe^{2+}. Reactions (20) and (22) have high rate constants, while that of (18), is low; (18) is, therefore, the rate determining step in the cycle. In the absence of further reactions, there is mutual balance among the rates of the reactions of the cycle; all rates are equal. Reactions (19) and (21) act as perturbations; they remove the carriers of the cycle: $HO_2\cdot$, $OH\cdot$ and Fe^{2+}. At the start of the reaction, the course involves both the steps of the kernel and the perturbations. Due to perturbations, the rate of the evolution of O_2 (22) will be less than the rate of production of free radicals (18), because a fraction of free radicals has been removed in perturbation reactions. In these reactions Fe^{2+} ions are oxidized to Fe^{3+}. As a result, $[Fe^{2+}]$ and the rate of initiation becomes lower. A new cycle will end with an additional amount of Fe^{2+} ions oxidized to Fe^{3+}. As the cycles are repeated, $[Fe^{2+}]$ will be reduced continuously until it will become negligible beside both $[H_2O_2]$ and $[Fe^{3+}]$. Perturbation reactions will then become insignificant and the course of the reaction will be reduced to reactions of the kernel. From this point on, O_2 will be evolved in a steady state at a constant and low $[Fe^{2+}]$; *the reaction will become a catalytic decomposition of H_2O_2*. With the existing rate constants, the rate of O_2 evolution in the initial phase, in spite of perturbation reactions, is high (measured on a timescale of seconds). In the catalytic phase in contrast, the reaction is slow, even on the timescale of minutes. This description explains the observed "initial burst of O_2", the amount of which is not identical with "the total amount of O_2 evolved in the Fenton reaction". It represents only the amount of gas evolved during the rapid phase. To calculate its magnitude theoretically, the rate equations of Barb et al. were integrated numerically using their rate constants and the value of $[O_2]$ was determined at a point where both conditions $v_{19}/v_{20} < 10^{-3}$ and $v_{21}/v_{22} < 10^{-3}$ were satisfied [4]. The results have shown a definite dependence of this value on $[H_2O_2]_o$ (Ref. [11], Figure 3). It is concluded, therefore, that the existence of an

upper limit in the amount of O_2 evolved in the Fenton reaction during the initial burst at high $[H_2O_2]$ has not been explained satisfactorily by the model of Barb et al [4].

A radical—radical reaction has also been suggested as the source of O_2 [20].

$$HO_2\cdot + HO_2\cdot \rightarrow O_2 + H_2O_2 \tag{23}$$

This reaction severs, however, the connection between O_2 evolution and the regeneration of Fe^{2+}, a phenomenon demonstrated experimentally (Ref. [4], p. 476). It is, therefore, unacceptable. The same applies also to the reaction

$$HO_2\cdot + OH\cdot \rightarrow O_2 + H_2O \tag{24}$$

This exhausts the possibilities of constructing mechanisms for the Fenton reaction based on free radicals.

6. Conclusions

There are three basic facts for which any mechanism of the Fenton reaction must account:

1. Change in the ratio of concentrations of the products when the ratio of concentrations of reactants is varied.
2. Coupling of the evolution of O_2 with the regeneration of Fe^{2+}.
3. The existence of an upper limit to the amount of O_2 formed when $[H_2O_2]$ is increased beyond a certain value. The mechanism of Haber and Weiss fails to explain all three points. The mechanism of Barb et al. explains points one and two but fails to explain point three [4]. The nonradical mechanism explains all three points.

Funding: The author received financial support for the research, authorship, and/or publication of this article; the research was supported by a grant from the Hebrew University for Emeriti. The help of Miss Ronnie Kremer with the artwork in Figure 1 is greatly appreciated.

Conflicts of Interest: The author declare no conflict of interest.

References

1. Pignatello, J.J.; Oliveros, E.; MacKay, A. Advanced oxidation processes for organic contaminant destruction based on the Fenton reaction and related chemistry. *Crit. Rev. Environ. Sci. Tech.* **2006**, *36*, 1–84. [CrossRef]
2. Burkitt, M.J. Chemical, Biological and Medical Controversies Surrounding the Fenton Reaction. *Prog. React. Kinet. Mech.* **2003**, *28*, 75–104. [CrossRef]
3. Haber, F.; Weiss, J. The catalytic decomposition of hydrogen peroxide by iron salts. *J. Proc. R. Lond. Ser. A* **1934**, *147*, 332–349.
4. Barb, W.G.; Baxendale, J.H.; George, P.; Hargrave, K.R. Reactions of ferrous and ferric ions with hydrogen peroxide. Part 1–the ferrous\ ion reaction. *Trans. Faraday Soc.* **1951**, *47*, 462–500. [CrossRef]
5. Bray, W.C.; Gorin, M.H. Ferryl ion, a compound of tetravalent iron. *J. Am. Chem. Soc.* **1932**, *54*, 2124–2125. [CrossRef]
6. Walling, C. Fenton's reagent revisited. *Acc. Chem. Res.* **1975**, *8*, 125–131. [CrossRef]
7. Walling, C. Intermediates in the Reactions of Fenton Type Reagents. *Acc. Chem. Res.* **1998**, *31*, 155–157. [CrossRef]
8. Goldstein, S.; Meyerstein, D.; Czapski, G. The Fenton Reagents. *Free Radical Biol. Med.* **1993**, *15*, 435–445. [CrossRef]
9. Dunford, H.B. Oxidations of iron(II)/iron(III) by hydrogen peroxide from aquo to enzyme. *Coord. Chem. Rev.* **2002**, *233–234*, 311–318. [CrossRef]
10. Kremer, M.L. Mechanism of the Fenton reaction. Evidence for a new intermediate. *Phys. Chem. Chem. Phys.* **1999**, *1*, 3595–3605. [CrossRef]
11. Kremer, M.L. New kinetic analysis of the Fenton reaction: Critical examination of the free radical–chain reaction concept. *Prog. React. Kinet. Mech.* **2019**, *44*, 289–299. [CrossRef]
12. Gallard, H.; de Laat, J.; Legube, B. Effect of pH on the Oxidation Rate of Organic Compounds by Fe^{II}/H_2O_2. Mechanisms and simulation. *New J. Chem.* **1998**, *22*, 263–268. [CrossRef]
13. de Laat, J.; Gallard, H. Catalytic Decomposition of Hydrogen Peroxide by Fe(III) in Homogeneous Aqueous Solution: Mechanism and Kinetic Modeling. *Environ. Sci. Technol.* **1999**, *33*, 2726–2732. [CrossRef]
14. Bossmann, S.H.; Oliveros, E.; Göb, S.; Siegwart, S.; Dahlen, E.P.; Payavan, L., Jr.; Straub, M.; Wörner, M.; Braun, A.M. New Evidence against Hydroxyl Radicals as Reactive Intermediates in the Thermal and Photochemically Enhanced Fenton Reactions. *J. Phys. Chem. A* **1998**, *102*, 5542–5550. [CrossRef]
15. Buda, F.; Ensing, B.; Gribnau, M.C.M.; Baerends, E. DFT Study of the Active Intermediate in the Fenton Reaction. *Chem. Eur. J.* **2001**, *7*, 2775–2783. [CrossRef]

16. Lu, H.F.; Chen, H.F.; Kao, C.L.; ChaO, I.; Chen, H.Y. A computational study of the Fenton reaction in different pH ranges. *Phys. Chem. Chem. Phys.* **2018**, *20*, 22890–22901. [CrossRef] [PubMed]
17. Rush, J.D.; Koppenol, W.H. The reaction between ferrous polyaminocarboxylate complexes and hydrogen peroxide: An investigation of the reaction intermediates by stopped flow spectrophotometry. *J. Inorg. Biochem.* **1987**, *29*, 199–215. [CrossRef]
18. Masarwa, A.; Rachmilowich-Calis, S.; Meyerstein, N.; Meyerstein, D. Oxidation of organic substrates in aerated aqueous solutions by the Fenton reagent. *Coord. Chem. Rev.* **2005**, *249*, 1937–1943. [CrossRef]
19. Kremer, M.L. Strong inhibition of the Fe^{3+} + H_2O_2 reaction by ethanol: Evidence against the free radical theory. *Prog. React. Kinet. Mech.* **2017**, *42*, 397–413. [CrossRef]
20. Perez-Benito, J.F. Iron (III)–Hydrogen Peroxide Reaction: Kinetic Evidence for a Hydroxyl–Mediated Chain Mechanism. *J. Phys. Chem. A* **2004**, *108*, 4853–4858. [CrossRef]